Ca2+ induces an extended conformation of the inhibitory region of troponin I in cardiac muscle troponin

ARTICLE *in* JOURNAL OF MOLECULAR BIOLOGY · DECEMBER 2001

Impact Factor: 4.33 · DOI: 10.1006/jmbi.2001.5118 · Source: PubMed

4 AUTHORS, INCLUDING:

Wen-Ji Dong
Washington State University
87 PUBLICATIONS **1,379** CITATIONS
SEE PROFILE

John M Robinson
South Dakota State University
40 PUBLICATIONS **481** CITATIONS
SEE PROFILE

Herb C Cheung
University of Alabama at Birmingham
132 PUBLICATIONS **3,211** CITATIONS
SEE PROFILE

doi:10.1006/jmbi.2001.5118 available online at http://www.idealibrary.com on IDEAL® J. Mol. Biol. (2001) 314, 51–61

JMB

Ca^{2+} Induces an Extended Conformation of the Inhibitory Region of Troponin I in Cardiac Muscle Troponin

Wen-Ji Dong*, Jun Xing, John M. Robinson and Herbert C. Cheung

Department of Biochemistry and Molecular Genetics University of Alabama at Birmingham, Birmingham AL 35294, USA

**Corresponding author*

The inhibitory region of troponin I (TnI) plays a central regulatory role in the contraction and relaxation cycle of skeletal and cardiac muscle through its Ca^{2+}-dependent interaction with actin. Detailed structural information on the interface between TnC and this region of TnI has been long in dispute. We have used fluorescence resonance energy transfer (FRET) to investigate the global conformation of the inhibitory region of a full-length TnI mutant from cardiac muscle (cTnI) in the unbound state and in reconstituted complexes with the other cardiac troponin subunits. The mutant contained a single tryptophan residue at the position 129 which was used as an energy transfer donor, and a single cysteine residue at the position 152 labeled with IAEDANS as energy acceptor. The sequence between Trp129 and Cys152 in cTnI brackets the inhibitory region (residues 130-149), and the distance between the two sites was found to be 19.4 Å in free cTnI. This distance was insensitive to reconstitution of cTnI with cardiac troponin T (cTnT), cTnC, or cTnC and cTnT in the absence of bound regulatory Ca^{2+} in cTnC. An increase of 9 Å in the Trp129-Cys152 separation was observed upon saturation of the Ca^{2+} regulatory site of cTnC in the complexes. This large increase suggests an extended conformation of the inhibitory region in the interface between cTnC and cTnI in holo cardiac troponin. This extended conformation is different from a recent model of the Ca^{2+}-saturated skeletal TnI-TnC complex in which the inhibitory region is modeled as a β-turn. The observed Ca^{2+}-induced conformational change may be a switch mechanism by which movement of the regulatory region of cTnI to the exposed hydrophobic patch of the open regulatory N-domain of cTnC pulls the inhibitory region away from actin upon Ca^{2+} activation in cardiac muscle.

Keywords: cardiac troponin I; inhibitory region; FRET; Ca^{2+} activation

Introduction

Contraction of vertebrate striated muscle is regulated by a set of Ca^{2+}-dependent interactions among the thin filament proteins, including the subunits of the heterotrimeric troponin, actin, and tropomyosin. Troponin C (TnC) is the Ca^{2+}-binding subunit of troponin, troponin I (TnI) is the inhibitory subunit which binds to actin to inhibit actomyosin ATPase and force development, and troponin T (TnT) binds to tropomyosin. Activation of ATPase and force begins with the binding of activator Ca^{2+} to the Ca^{2+}-specific sites located at the N-terminal half of TnC, and this binding weakens the interaction between TnI and actin, thus relieving the inhibition of ATPase and force gener-

Abbreviations used: Tn, troponin; TnC, troponin C; TnI, troponin I; TnT, troponin T; c, cardiac muscle; fs, fast skeletal muscle; cTnI(129W/152C), mutant cTnI(C81S/C98I/L129W/A152C/W192F); FRET, fluorescence resonance energy transfer; DTT, dithiothreitol; Mops, 3-(*N*-morpholino)propanesulfonic acid; EGTA, ethylene glycol-bis-(β-aminoethyl ether)-*N*,*N*,*N*′,*N*′-tetraacetic acid; IAEDANS, 5-(iodoacetamidoethyl)aminonaphthalene-1-sulfonic acid; GuHCl, guanidine hydrogen chloride.

E-mail address of the corresponding author: wdong@uab.edu

0022-2836/01/010051–11 $35.00/0

ation, and promotes an enhanced interaction between TnI and TnC. The crystal structures of fast skeletal muscle TnC (fsTnC) show a dumbbell-shaped molecule with two globular domains separated by an extended, solvent-exposed central helix.[1–3] The N-terminal domain has two Ca^{2+}-specific sites (sites I and II), which bind Ca^{2+} with a low affinity ($K_a \sim 10^5$ M^{-1}), and the C-terminal domain has two high-affinity Ca^{2+} binding sites (sites III and IV, $K_a \sim 10^7$ M^{-1}), which also bind Mg^{2+} competitively ($K_a \sim 10^3$ M^{-1}). Ca^{2+} binding to the two sites in the N-domain is believed to be the key step to initiate contraction by modulating the interactions between TnI and actin and TnC. Structurally, these interactions arise from a Ca^{2+}-induced opening of the regulatory N-domain of TnC and an exposure of a hydrophobic patch in this domain for an enhanced interaction between TnI and TnC. In cardiac muscle TnC (cTnC), the site I cannot bind Ca^{2+} due to substitutions of two critical amino acids and an insertion in the binding loop. Saturation of the site II in cardiac muscle is necessary and sufficient to trigger contraction.[4] Recent studies have shown that bound cTnI is a prerequisite to achieve a Ca^{2+}-induced structural opening of the regulatory N-domain of cTnC to an extent similar to that previously observed for fsTnC in the absence of bound fsTnI.[5–6] These findings have raised the question as to whether there are substantial mechanistic differences in the regulatory processes of the two types of striated muscle.

In rabbit fsTnI, the segment between residues 96-116 (inhibitory region) was identified from proteolytic fragments as the site for actin binding, and this binding which occurred in relaxed muscle was largely responsible for full inhibition of ATPase.[7] Within this region, the minimal sequence that caused inhibition was subsequently localized to residues 104-115.[8] Thus, the fsTnI sequence between residues 96-115 is regarded as the inhibitory region. The corresponding inhibitory region in cTnI is between residues 130-149 because cTnI has a unique N-terminal extension. When the Ca^{2+}-specific sites of fsTnC are saturated, the inhibitory region switches from actin to a site in fsTnC which has not been clearly defined. A contiguous segment (the Ca^{2+}-dependent interaction site with TnC, residues 116-131 in fsTnI and residues 150-165 in cTnI) then moves to the Ca^{2+}-loaded open regulatory N-domain of TnC and binds to the exposed hydrophobic pocket. Since the inhibitory region plays a pivotal role in the inhibition and activation of muscle functions, knowledge of its conformations in troponin with and without bound activator Ca^{2+} is of basic importance in our understanding of the entire trigger mechanism of contraction.

Several studies have been reported to examine the global shape of fsTnI in binary and ternary complexes with the other troponin subunits. One study based on small-angle neutron scattering data proposed an extended conformation for the complex in which fsTnI spirally wraps around the length of fsTnC,[9] suggesting extensive contacts between the two proteins. A second model, also based on scattering data, represented fsTnI in the complexes by two non-coaxial ellipsoid of revolutions.[10] These models do not show structural features of specific regions of fsTnI in the complexes. Photo-crosslinking and FRET data were used to construct a map showing proximity relationship of fsTnI with fsTnC in their complex,[11] and an atomic model of fsTnC was used as a scaffold for several contiguous segments of fsTnI to develop a model of the fsTnI-cTnC complex at atomic resolution.[12] The latter two models provided a view of the inhibitory and other regions of fsTnI in the fsTnI-fsTnC complex.

We previously reported an investigation of the global conformation of cTnI, both free and bound to cTnC, using FRET and by determination of sulfhydryl reactivity of cysteine residues located along the length of the cTnI molecule.[13] Our general conclusion was that cTnI has an extended conformation and remains extended upon complex formation with cTnC. In the complex, several segments were found to be more extended than in free cTnI. Here, we have extended the cTnI studies by focusing on the global conformation of a cTnI segment that includes the inhibitory region. Results from the determination of intersite distance indicate a large Ca^{2+}-induced increase in the distance in the inhibitory region. This global conformational change provides new insights into the mechanistic role of the inhibitory region as a molecular switch in Ca^{2+} activation of cardiac muscle.

Results

Fluorescence properties of cTnI mutant

The segment of interest in the cTnI mutant is between Trp129 and Cys152, which bracket the inhibitory region (residues 130-149). The fluorescence of Trp129 was characterized by both the steady-state and time-resolved methods. These results are summarized in Table 1. In the presence of 6 M GuHCl, the fluorescence quantum yield (Q) was 0.11 and the maximum emission wavelength (λ_{max}) was 347 nm. The fluorescence intensity decay was biexponential with a weighted mean lifetime of 3.15 ns. These parameters are comparable to those for NATA (*N*-acetyl-L-tryptophanamide) determined in aqueous solution (quantum yield 0.14, maximum emission at 353 nm, and weighted mean lifetime 3.18 ns), suggesting an exposed environment of Trp129 in denatured cTnI. In the absence of GuHCl, the quantum yield increased to 0.16 with the emission maximum blue shifted to 334 nm. The intensity decay became triexponential, and the weighted mean lifetime increased to 4.19 ns. In the binary complex with the tryptophanless cTnT, the fluorescence properties of the Trp129 of cTnI were not affected, suggesting negligible interaction between the

Table 1. Fluorescence emission parameters of Trp129 in cTnI (129W/152C) mutant

Sample[a]	λ_{max}(nm)	Q	Life times(ns)			$\langle\tau\rangle$ (ns)
cTnI in GuHCl	347.0	0.11	3.94 (0.44)	1.79 (0.39)		3.15
cTnI	334.1	0.16	5.36 (0.39)	2.04 (0.39)	0.18 (0.31)	4.19
cTnI-cTnT	334.0	0.16	4.97 (0.40)	1.73 (0.35)	0.21 (0.25)	4.13
cTnI-cTnC + Mg^{2+}	334.1	0.16	6.47 (0.17)	3.02 (0.46)	0.83 (0.33)	4.18
cTnI-cTnC + Ca^{2+}	329.0	0.26	6.32 (0.21)	3.51 (0.48)	1.65 (0.31)	4.31
cTn + Mg^{2+}	335.0	0.21	5.29 (0.51)	2.06 (0.49)		4.41
cTn + Ca^{2+}	331.0	0.30	4.81 (0.89)	1.63 (0.11)		4.68

[a] The first sample was cTnI in 6 M GuHCl, and the other samples were cTnI and its complexes with cTnT (cTnI-cTnT), cTnC (cTnI-cTnC), and both cTnT and cTnC (cTn). λ_{max} is the wavelength of maximum emission and Q is the quantum yield. The intensity decay of the Trp129 in some samples were biexponential with two lifetimes, and in other samples were triexponential with three lifetimes. The number in parentheses was the fractional amplitude (α_i) associated with the ith lifetime. $\langle\tau\rangle$ is the intensity-weighted mean life time calculated from $\langle\tau\rangle = \Sigma\alpha_i\tau_i^2/\Sigma\alpha_i\tau_i$.

N-terminal end of the inhibitory region of cTnI with cTnT. The relatively low quantum yield in the complex was indicative of an exposed environment of Trp129, although this exposure was less than in the denatured state of free cTnI.

In the absence of bound regulatory Ca^{2+}, the Trp129 fluorescence properties of cTnI in cTnI-cTnC were very similar to those for free cTnI, although there were differences in the three decay components. The weighted mean lifetimes were, however, the same. Saturation of the regulatory site of cTnC in the complex, however, induced a 62 % increase in quantum yield, a 5 nm blue shift of the emission maximum, and an increase in the mean lifetime. In the ternary complex with cTnC and cTnT, bound Ca^{2+} at the regulatory site of cTnC resulted in a further increase in quantum yield to 0.30 and an increase in the mean lifetime to 4.68 ns. A simple interpretation of these data is that a segment of the cTnI inhibitory region in troponin senses considerable environmental changes during the transition of the regulatory N-domain of cTnC from the apo state to the holo state. These changes resulted from multiple interactions among the three troponin subunits.

Fluorescence resonance energy transfer

The fluorescence emission spectrum of Trp129 in cTnI mutant (129W/152C) is a broad single band (spectrum not shown) with the emission peak at 334.1 nm (Table 1). Figure 1 shows the emission spectra of this mutant in which AEDANS was linked to Cys152 as the energy acceptor upon excitation of the donor tryptophan residue. The band in the 330 nm region is the donor tryptophan emission, and the other band in the 480-nm region is sensitized acceptor emission. The intensity of the tryptophan band shown in Figure 1(a) (curves 1 and 2) was considerably smaller than that determined without the presence of the acceptor. The large quenching of the tryptophan band and the concomitant appearance of an intense acceptor emission band (Figure 1(a), curves 1 and 2) clearly indicate a significant fluorescence energy transfer from Trp129 to the acceptor AEDANS attached to Cys152. The transfer was essentially the same for isolated cTnI (curve 1) and the binary complex cTnI-cTnT (curve 2). Formation of the binary complex had no structural effect on the inhibitory region where Trp129 was located. When cTnI was denatured, the energy transfer efficiency was dramatically decreased as evident from an increase of the donor band with a red shift, and a large decrease of the sensitized acceptor band (Figure 1(a), curve 3). In unfolded cTnI the donor-acceptor separation increased significantly thereby reducing the transfer between the two sites. The two lower panels in Figure 1 show the effect of bound Ca^{2+} at the regulatory site of cTnC on energy transfer which occurred between the two sites in cTnI in the binary (Figure 1(b)) and ternary (Figure 1(c)) complexes. This effect was a large increase in donor emission and a reduction of the sensitized acceptor emission (curves 2 *versus* 1). The reduction in Ca^{2+}-induced energy transfer suggested a large increase in the separation between donor and acceptor sites.

To quantitatively determine changes in intersite distance, time-resolved fluorescence data were collected for each experimental condition. Figure 2 shows representative intensity decays of the donor tryptophan in the absence and the presence of the acceptor. In the presence of the acceptor (curve 2), the data showed a rapid initial decay when compared with the data obtained without the acceptor (curve 1). In the complex cTnI-cTnT, the donor-alone decay (curve 3) was essentially the same as that for isolated cTnI, and the extent of energy transfer in the complex (curve 4) was little affected. These and other time-resolved energy transfer data were quantified as distributions of the distances between donor and acceptor, and these distributions are shown in Figure 3. The distance parameters recovered from the distributions are listed in Table 2. Except for denatured cTnI (curve 2), the distributions of the Trp129-Cys152 distances fall into two groups. The mean distances of the first group of four distributions were clustered within the narrow range 19.1-19.9 Å, with half-widths in

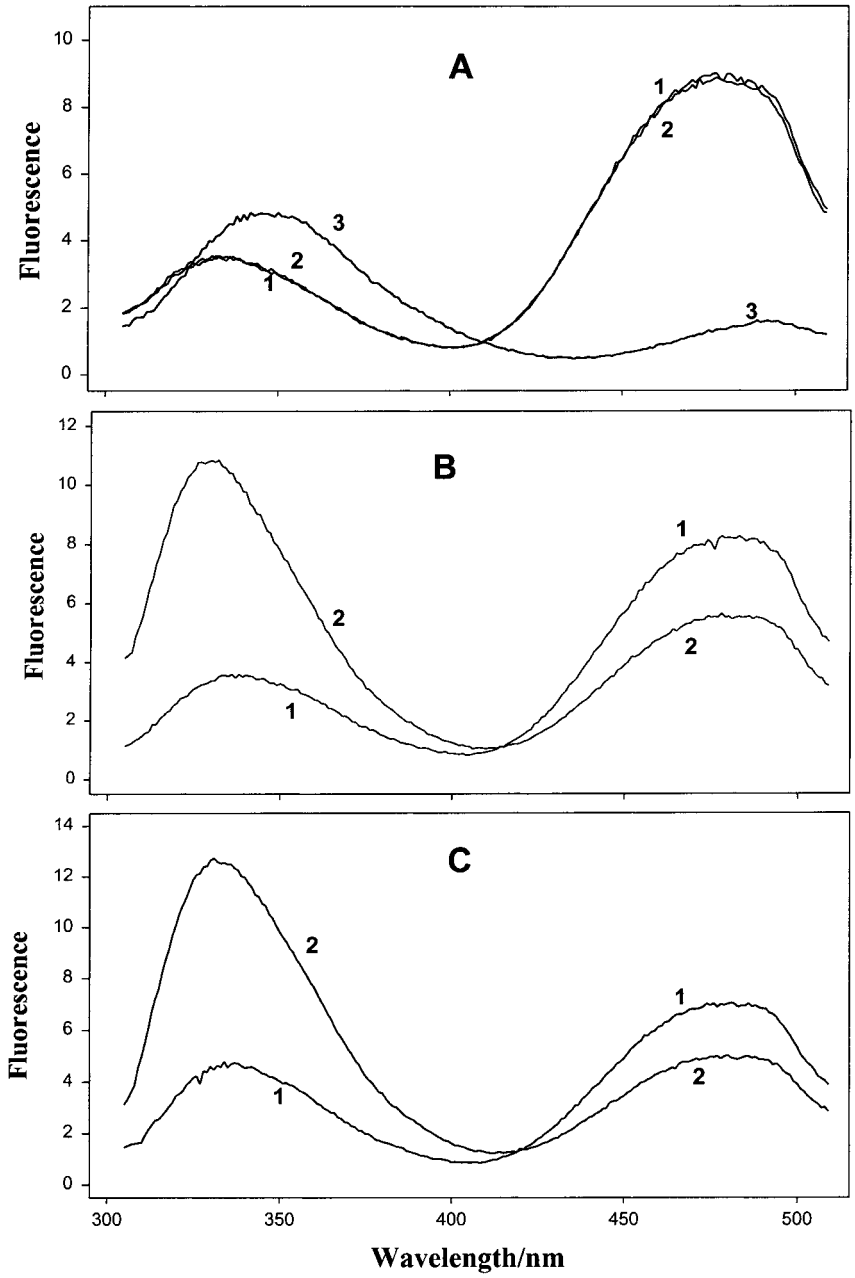

Figure 1. Steady-state fluorescence emission spectra of the single-tryptophan mutant cTnI(129W/152C) labeled at Cys152 with IAEDANS. (a) Curve 1, free cTnI; curve 2, cTnI complexed with cTnT; curve 3, denatured cTnI (6 M GuHCl). (b) cTnI-cTnC complex: curve 1, in the presence of Mg^{2+} (sites III and IV in cTnC were saturated with Mg^{2+}, and the regulatory site II was unoccupied); curve 2, in the presence of Ca^{2+} (regulatory site II in cTnC was saturated). (c) reconstituted cTn: curve 1, in Mg^{2+}; curve 2, in Ca^{2+}. See the text for conditions.

the range 4.1-5.4 Å for three of the distributions and 6.9 Å for the fourth distribution. The smaller half-width values suggested relatively little conformational fluctuation in the cTnI segment between the donor and acceptor sites. The donor-acceptor distance of the 129-152 segment of cTnI was not influenced by bound cTnC or cTnT in the absence of bound regulatory Ca^{2+}. The other group of two distributions showed mean distances of 28.5 and 29.4 Å with essentially the same values of the half-width. The mean distances of the second group of distributions were about 9 Å longer than those of the first set of distributions and resulted from the presence of bound regulatory Ca^{2+} in the cTnC of the two complexes. The 6.9 Å half-width for the distribution of the binary complex in the absence bound Ca^{2+} at the regulatory N-domain of cTnC was reduced by 2.1 Å upon saturation of the regulatory site. These results suggested a large Ca^{2+}-dependent conformational change of the inhibitory region of cTnI within cardiac troponin. In the binary cTnI-cTnC, this conformational change not only reflected movement of the donor and acceptor sites away from each other, but also reduced the flexibility of the segment connecting the two sites. In the ternary complex without bound activator Ca^{2+}, the segmental flexibility was already reduced, and the effect of bound regulatory Ca^{2+} on the flexibility was relatively negligible. The broad distribution of the distances in the presence of GuHCl (curve 2, half-width 8.8 Å) reflected an unstructured flexible segment in which the two ends moved away from each other.

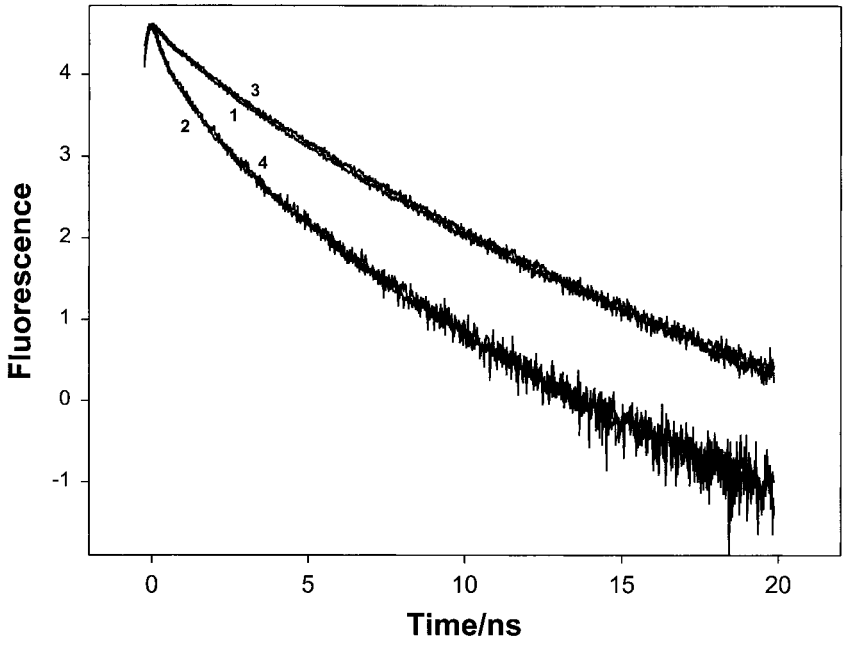

Figure 2. Representative fluorescence intensity decays of donor Trp129 in mutant cTnI(129W/152C) and its complexes with cTnT. (1) Free cTnI in the absence of energy acceptor; (2) free cTnI in the presence of energy acceptor AEDANS linked to Cys152. (3) cTnI-cTnT in the absence of energy acceptor, and (4) cTnI-cTnT in the presence of acceptor. Protein concentration was 10 μM.

The two parameters of the distance distribution, *r* and *hw*, are strongly correlated. To examine the extent to which the mean distances recovered from the data obtained from the complexes in the absence of bound regulatory Ca^{2+} can be distinguished from those recovered from the complexes in the presence of bound Ca^{2+}, the χ^2_R surfaces of the mean distances were constructed.[14,15] The two surfaces for the mean distance of the apo and holo states of the binary and ternary complexes are shown in Figure 4. The range of mean distance consistent with the data is defined by the value of χ^2_R (variance ratio) in the surface with random noise in 68 % of repetitive measurements (one standard deviation). For both complexes, the two surfaces are clearly well separated and intersect at normalized χ^2_R values that are three- to fourfold elevated above the one standard deviation value. The two mean distances (19.9 and 28.5 Å) for the binary complex and the two mean distances (19.8 and 29.4 Å) for the ternary complex are significantly different from each other. It may not be immediately apparent that these variance ratio surfaces are not symmetric, and it is not appropriate to assign a symmetric uncertainty to a mean distance value.

Anisotropy decays

In the calculation of the mean distances from the distributions of the distances, the orientation factor κ^2 was assumed to be two-thirds for isotropic and rapid tumbling of the fluorophores. If the values of κ^2 differed significantly in the apo and holo states of cTnI-cTnC and cTn, it would be difficult to compare the calculated mean distances for the two states. The difference in κ^2 cannot be quantitatively determined, but the potential contribution of a change in κ^2 can be assessed from the axial depolarization factors of donor and acceptor.[16] Anisotropy decay measurements were made on both the donor tryptophan and the acceptor probe AEDANS attached to Cys152. The limiting aniso-

Table 2. Parameters for the distance Trp129-Cys152 in cTnI

Sample[a]	$\langle d^x_d \rangle$	$\langle d^x_a \rangle$	κ^2_{max}	κ^2_{min}	R_o(Å)	*hw*(Å)	*r*(Å)
cTnI in GuHCl	0.69	0.62	2.40	0.23	20.8	8.8	26.4
cTnI	0.86	0.70	2.91	0.15	23.0	5.4	19.4
cTnI-cTnT	0.80	0.72	2.83	0.16	21.9	4.1	19.1
cTnI-cTnC + Mg^{2+}	0.91	0.70	3.01	0.13	21.9	6.9	19.9
cTnI-cTnC + Ca^{2+}	0.93	0.68	3.00	0.13	23.6	4.8	28.5
cTn + Mg^{2+}	0.86	0.70	2.91	0.15	22.8	5.0	19.8
cTn + Ca^{2+}	0.91	0.70	3.01	0.13	24.5	4.6	29.4

[a] The samples were the same as those described for Table 1. The axial depolarization factors for the donor and acceptor are $\langle d^x_d \rangle$ and $\langle d^x_a \rangle$, respectively. κ^2_{max} and κ^2_{min} define the upper and lower limits of the orientation factor κ^2 calculated from the axial depolarization factors. In these calculations, the fundamental anisotropy for donor tryptophan was taken to be 0.232 and that for the acceptor probe AEDANS was taken to be 0.37. R_o is the Förster critical distance at which the transfer efficiency is 0.5. *hw* is the half-width of the distribution of the distances and *r* is the mean distance recovered from the distribution of the distances using $\kappa^2 = 2/3$.

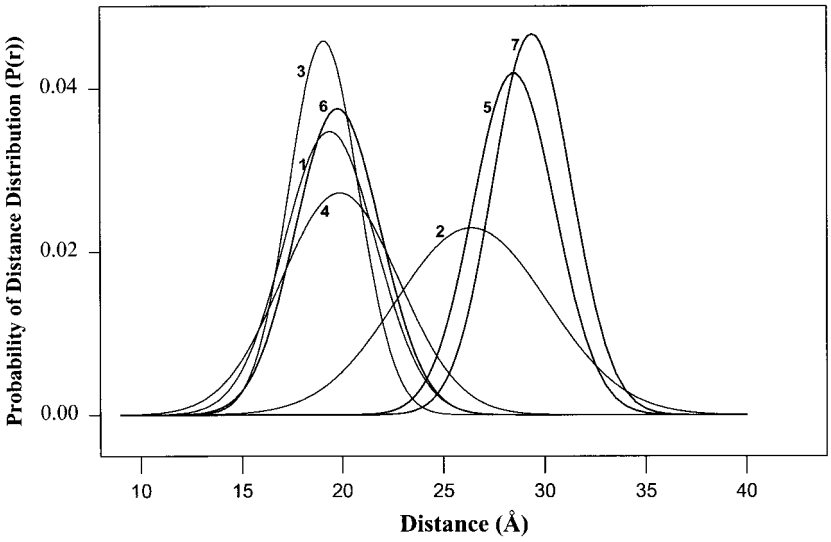

Figure 3. Area-normalized distributions of intersite distances between Trp129 and Cys152 of cTnI(129W/152C). Curve1, cTnI; curve 2, denatured cTnI in 6 M GuHCl; curve 3, cTnI-cTnT; curve 4, cTnI-cTnC + Mg^{2+}; curve 5, cTnI-cTnC + Ca^{2+}; curve 6, cTn + Mg^{2+}; curve 7, cTn + Ca^{2+}. The distributions were calculated from intensity decay data similar to those shown in Figure 2, using the program CFS_LS/GAUDIS.[28]

tropies of donor and acceptor were determined from the decay profiles, and these values were used to calculate the depolarization factors and the lower and upper limits of κ^2 (κ^2_{min} and κ^2_{max}). These results are also listed in Table 2. The differences in depolarization factors between the apo and holo states for both binary and ternary complexes were very small, suggesting very similar probe orientations in both states. The range of κ^2 is essentially the same for both states. These properties of donor and acceptor suggested that the contribution of potential differences in κ^2 to the observed changes in energy transfer between the apo and holo state was minimal and the observed changes in energy transfer reflected predominantly changes in donor-acceptor separation.

Discussion

The Ca^{2+}-induced interaction between TnC and TnI is the key trigger step in striated muscle contraction and has long been a major focus in many laboratories. These two proteins are involved in molecular switching in the relaxation and contraction cycle, are subunits of the troponin complex, and have multiple domains. To elucidate this switching mechanism, it is necessary to understand both intersubunit interactions within troponin as well as intradomain structural rearrangements. In the absence of bound regulatory Ca^{2+} (relaxed muscle), the N-terminal segment of TnI (fsTnI residues 1-40, or cTnI residues 32-73) has been shown to bind to the C-terminal domain of TnC, and the inhibitory region to bind to actin. The binding of regulatory Ca^{2+} to TnC switches the TnI inhibitory region away from actin, thus relieving the inhibition. The released inhibitory region is believed to bind to a site in TnC. This site has not been unequivocally demonstrated, although short peptides have been used previously to localize the site. Since short peptides are known to bind to multiple regions of TnC depending upon conditions, these studies yielded disparate results suggesting interactions of the inhibitory region with either the C-domain, both globular domains, or the central helix of TnC.[17–20] NMR studies indicated that an inhibitory peptide corresponding to rabbit fsTnI residues 104-115 bound to fsTnC had a hairpin conformation,[21] but a longer bound peptide (residues 96-115) had an extended conformation.[22] A recent NMR study showed that the cTnI inhibitory peptide (residues 129-147) bound to the N-domain and weakly to the central helix of cTnC, but not to the C-domain if cTnC was first saturated in its C-domain with the cTnI N-terminal peptide residues 1-80.[23] These and other similar studies have made clear that use of short peptides to model the inhibitory region of TnI in troponin are problematic because the peptide results may not be physiologically relevant.

We have used FRET to determine the separation between two residues which bracket the cTnI inhibitory region (residues130-149) of a full-length cTnI mutant reconstituted into binary complexes and the trimeric troponin complex. The two residues are Trp129 and Cys152. The distribution of the intersite distances is not influenced by formation of binary complexes, or reconstitution of cTnI into cTn. The mean distances are within a narrow range for free cTnI, cTnI-cTnT, and the other complexes in which the single Ca^{2+} regulatory site is not occupied. The distribution is shifted, however, toward longer distances with the mean intersite distance being 9 Å longer when the cTnC regulatory site in the complexes is saturated by Ca^{2+}. This large Ca-induced distance increase reflects a more extended conformation of the cardiac inhibitory region, and this large global conformational change of a critical cTnI segment has not been previously observed. This change may facili-

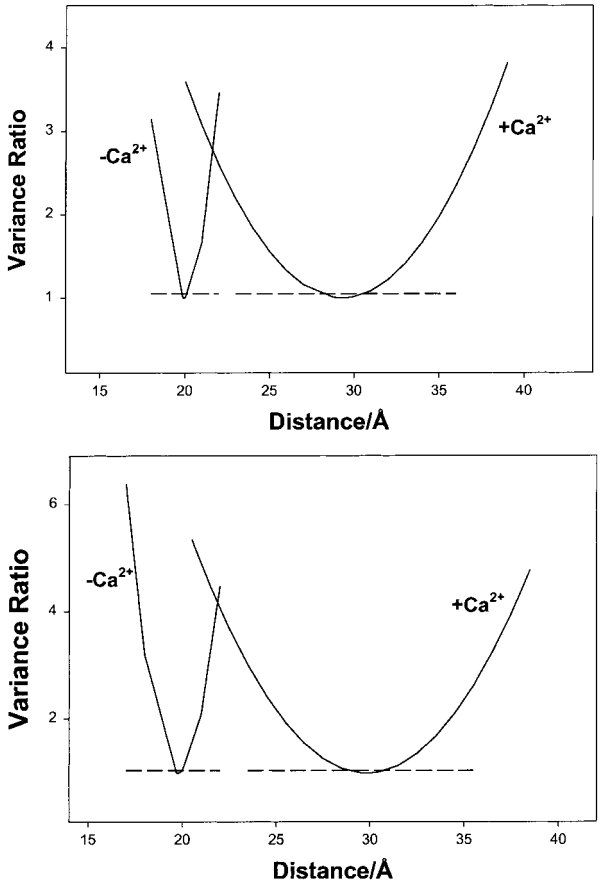

Figure 4. Dependence of the variance ratio (χ^2_R values normalized to the minimum value) on the mean distance for the distributions of the distances shown in Figure 3. Upper panel, cTnI-cTnC; lower panel, reconstituted cTn. In the calculation, the value of the mean distance was fixed at the value indicated on the horizontal axis, and the half-width was varied to minimize χ^2 values. The horizontal line indicates the statistically significant elevation of the variance ratio at the 68% confidence level.

tate movement of the contiguous cTnI regulatory region (residues 150-165) to the open regulatory N-domain of cTnC. It is not known whether the bound regulatory region also experiences global conformational changes.

The FRET results present a different view of the conformation of the inhibitory region of cTnI in Ca^{2+}-loaded cardiac troponin from a recent fsTnI-fsTnC model in which the skeletal inhibitory segment (residues 95-114, corresponding to cTnI residues 129-148) is modeled as a flexible β-hairpin.[12] As shown in Figure 5, the cardiac and skeletal inhibitory regions are highly homologous, which would suggest a similar β-turn for the cTnI inhibitory region in cardiac troponin. The proposed hairpin for fsTnI-fsTnC is based in part on the similarities between the sequence of the fsTnI inhibitory region and that of a β-hairpin region in profilin in which the hairpin is at the profilin/actin interface in the crystal structure of the profilin/actin complex. Residues Met95 and Ala118 of the model are in close proximity (Figure 6(a)) and the distance between the C^{α} atoms of these two residues is approximately 13 Å. The corresponding residues in cTnI are 129 and 152 (Figure 6(b)). If the entire segment between these two residues in cTnI was a-helical, its length would be approximately 35 Å. The observed donor-acceptor separation between Trp129 and Cys152 labeled with AEDANS in cTnI is approximately 20 Å, consistent with secondary structure prediction of a coil conformation in the middle of this segment (Figure 5). This distance is essentially the same for binary and ternary complexes in the absence of bound regulatory Ca^{2+}, and increases to *ca* 29 Å in the Ca^{2+}-loaded complexes (Figure 6(c)). The distances observed with the Ca^{2+}-loaded cardiac complexes are a factor of 2 longer than would be expected for a similar β-turn inhibitory segment (fsTnI residues 95-118) from the model of the Ca^{2+}-loaded skeletal binary complex. These large FRET distances are not compatible with a β-turn for the cTnI inhibitory region in cardiac troponin, regardless of whether the regulatory site in cTnC is saturated.

Although the absolute FRET distances may contain uncertainties that are not easily determined due to the orientation factor and the size of both donor and acceptor fluorophores, we showed that the axial depolarization factors of donor and acceptor are relatively unchanged when the cTnC regulatory site is saturated. This information suggests similar average probe mobilities in the two states and the observed difference in energy transfer between the two states reflects changes in intersite separation. In a previous FRET study using the same donor-acceptor pair as in the present work,[5] we found that donor-acceptor distances in the regulatory N-domain of cTnC in free cTnC and cTnC-cTnI were remarkably similar to the distances between C^{α} atoms of the same pairs of residues determined from the NMR solution structures of cTnC and cTnC bound to a cTnI peptide.[6] Our experience with previous FRET results lends credence to the conclusion of a large Ca^{2+}-induced increase in the separation between the two ends of the cardiac inhibitory region.

The segment (residues 129-152) of cTnI containing the inhibitory region is helical at both ends with a coil motif in the middle region, as suggested by secondary structure prediction (Figure 5). In spite of a coil motif, this segment is not very flexible in complexes with or without bound regulatory Ca^{2+}, as indicated by the relatively narrow distributions of the end-to-end distances with small half-widths (4-5 Å). The lack of a substantial flexibility is supported by the observation of a broad distribution of the distances for denatured cTnI with a longer mean distance (26.4 Å) and a larger half-width (~9 Å). This helix-loop-helix feature in cTn is not likely very extended in the absence of bound regulatory Ca^{2+}, but becomes

```
                125 130         140         150         160  165  170  174  180  185
cTnI            EIALTQKIYDLRGKFKRPTLRRVRISADAMMQALLGTRAKESLDLRAHLKQVKKEDIEKE

                92  96  100         110         120         130         140         150
fsTnI           LEDMNQKLFDLRGKFKRPPLRRVRMSADAMLRALLGSKHKVCMDLRANLKQVKKEDTEKE
                HHHHHHHCCCCCCCCCCCHHHHHHHHHHHHHHCCCCHHHHHHHHHHHHHHHHHHHHHHH
```

Figure 5. Local sequence alignment of mouse cTnI with rabbit fsTnI. The two sequences are aligned in the inhibitory region (double underlined), residues 130-149 of cTnI and residues 96-115 of fsTnI. The sequence in cTnI studied by FRET in the present work is also underlined (residues 129-152). The secondary structure predicted for the fsTnI sequence is shown below the sequence; it is a consensus derived from several methods and is taken from Tung *et al.*[12] The region with residues 150-165 in cTnI (fsTnI residues 116-131) is the site for the Ca^{2+}-dependent interaction with cTnC at the exposed hydrophobic pocket in the open N-domain (the cTnI regulatory region). The region with residues 174-182 in cTnI (fsTnI residues 140-148) is a second binding site for actin-tropomyosin.

considerably more extended when the single cTnC regulatory site is saturated. The representation of the cardiac inhibitory region as a linear segment with both helical and coil motifs is in agreement with the model described by Luo *et al.*[11]

We propose that the cTnI inhibitory region (residues 130-149) in cTn has an extended conformation with a large curvature (Figure 6(b)). This global conformation is supported by our previous FRET and sulfhydryl reactivity studies which suggested an extended cTnI polypeptide in cTn.[13] When Ca^{2+} binds to the regulatory site in cTnC, movement of the adjacent regulatory region (residues150-165) to the exposed hydrophobic pocket of the open regulatory N-domain of cTnC is facilitated by a global conformational change of the inhibitory region in which the curvature is reduced leading to a ''stretching'' of the ''end-to-end'' distance of the inhibitory region and a more extended conformation of the segment (Figure 6(c)). If the loop of the inhibitory region depicted in Figure 6(b) is the binding site for actin in relaxed muscle, then the

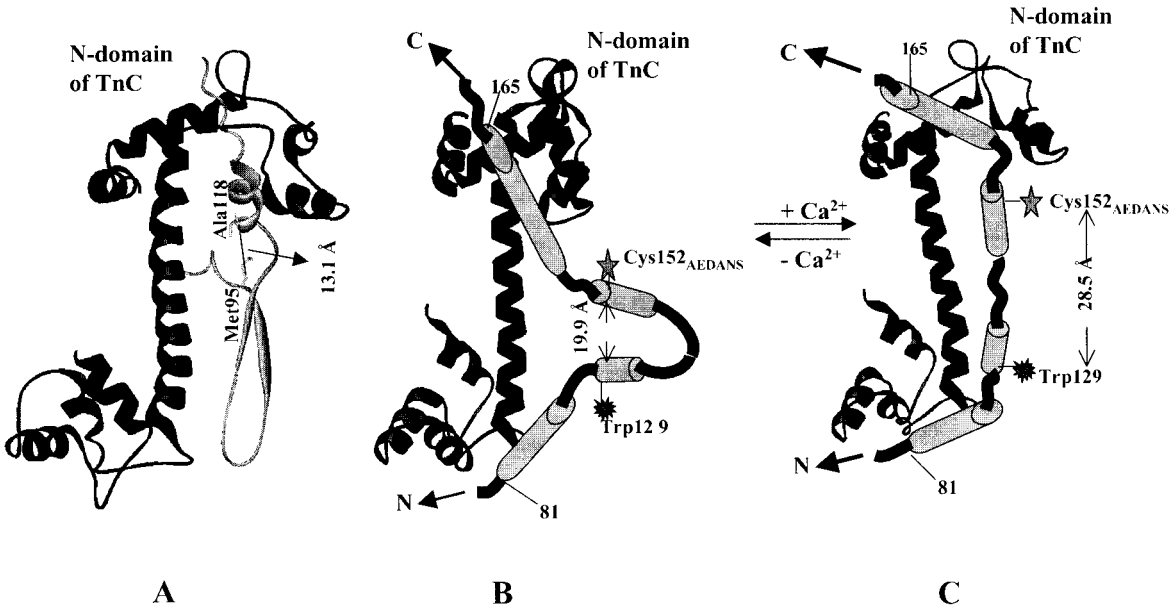

Figure 6. A model for the Ca^{2+}-induced conformational transition of the troponin I inhibitory region in cardiac troponin. Shown are schematic proximity relationships between cTnC (black) and cTnI (grey) arranged in an antiparallel fashion (B and C). cTnT is omitted. (a) A model of the conformation of the fsTnI inhibitory region in Ca^{2+}-loaded fsTnI-fsTnC from Tung *et al.*[12] (PDB accession code 1EW7), shown here for comparison with the present results for the cTnI inhibitory region. The fsTnI inhibitory region is shown as a hairpin from residues 95 to 114. The distance between the C^{α} atoms of Met95 and Ala118 is 13.1 A. (b) and (c), cTnI-cTnC in which residues 81-165 are shown for cTnI. Grey cylinders denote helices. The segment Trp129-Cys152 brackets the inhibitory region (residues 130-149) and corresponds to the fsTnI segment between Met95 and Ala118 shown in (a). cTnI residues 150-165 represent the regulatory region. The cTnI inhibitory segment is shown in (b) as a helix-loop-helix motif with an observed FRET distance of 19.9 Å between Trp129 and Cys152 in the absence of bound regulatory Ca^{2+} in cTnC. (c) shows binding of the cTnI regulatory region in the Ca^{2+}-loaded regulatory N-domain of cTnC and the conformation of the inhibitory segment Trp129-Cys152: the helix-loop-helix motif adopts an extended conformation with a separation of 28.5 Å between the two sites in cTnI-cTnC and 29.4 Å in cTn.

stretching of the loop induced by regulatory Ca^{2+} would allow the inhibitory region to pull away from actin and would serve as a structural switch between actin and cTnC to facilitate binding of the regulatory region to the N-domain of cTnC. The donor-acceptor distance of the extended segment from residues 129 to 152 is ~30 Å, comparable to the length of the central helix of TnC. It is plausible that the inhibitory region is positioned along the central helix,[12] but FRET results indicate that its conformation in this position is an extended segment rather than a β-turn. The interaction between cTnC and the inhibitory and regulatory regions of cTnI was investigated by multidimensional heteronuclear NMR.[24] This was accomplished by using a preparation of cTnC pre-saturated in its C-terminal domain with a cTnI peptide corresponding to residues 1-80, and a long cTnI peptide containing both the inhibitory and regulatory regions (residues 129-166). The results indicate that, in the presence of bound regulatory Ca^{2+}, the cTnI inhibitory segment (residues 129-147) does not interact specifically with the region of the central helix of cTnC and does not displace the bound N-terminal peptide (residues 1-80) of cTnI from the C-domain of cTnC. The long cTnI peptide served as a better model to study the inhibitory region than short inhibitory peptides because the conformation of the inhibitory region in the longer peptide can be modulated by the adjacent regulatory region. In a preliminary report,[25] the separations between residue 89 located in the central helix of cTnC and two residues within the inhibitory region of cTnI in cTnC-cTnI were determined to be greater than 30 Å. These distances decreased by only 3-4 Å in the presence of bound regulatory Ca^{2+}. These large separations are consistent with weak or no specific interactions between the cTnC central helix and the inhibitory region of cTnI, even in the presence of bound regulatory Ca^{2+}, as demonstrated by NMR.[24] When both FRET and NMR results are taken together, the extended inhibitory region in free holo cTn appears not to have specific interactions with the central helix and does not displace the bound N-terminal segment of cTnI from the C-domain of cTnC.

In summary, we have presented evidence for an extended inhibitory region of cTnI in Ca^{2+}-saturated cardiac troponin. This extended conformation results from a large Ca^{2+}-induced increase in the distance between the two ends of the inhibitory region. The transition from a less extended to a more extended conformation may be a switch mechanism to accommodate movement of the adjacent regulatory region toward the open regulatory N-domain of cTnC and to pull the inhibitory region away from actin. Thus, the conformation of cTnI inhibitory region is modulated by the regulatory region. Studies of the kinetics of the conformational changes of the cTnI regulatory segment reported here and of potential global conformational changes of the regulatory segment will provide further understanding of the role of these regions of cTnI in Ca^{2+} activation of cardiac muscle.

Materials and Methods

Protein preparation

Wild-type recombinant cTnC was over-expressed in *Escherichia coli* strain BL21(DE3) cells (Invitrogen) and purified as described.[5,26] Recombinant cTnT was generated from a full-length rat cTnT clone subcloned into a pET-17b vector. The plasmid was transformed into BL21(DE3) and expressed under isopropyl-1-thio-D-galactopyranoside induction. The plasmid was also used as a template to construct a tryptophanless cTnT mutant in which the two endogenous tryptophan residues at position 237 and 288 were converted into phenylalanine residues. The sequences of the cDNA clones were verified by sequence analysis. Overexpressed cTnT was isolated by ammonium sulfate fractionation at 42.5 and 60% saturation in a DEAE buffer containing 6 M urea, 25 mM Tris at pH 8.0, 1 mM EDTA and 0.5 mM DTT. A DEAE Fast Flow column was used to purify the cTnT with a NaCl gradient from 0.1 M to 0.4 M. The pooled cTnT fractions were then loaded on a SP column in a buffer containing 6 M urea, 50 mM sodium acetate at pH 5.3, 1 mM EDTA and 0.5 mM DTT, and the cTnT was eluted with a NaCl gradient from 0 to 1 M. Purified cTnT was dialyzed against 0.5% formic acid and lyophilized.

A mouse cDNA clone of cTnI was used to generate a mutant cTnI containing a single tryptophan residue and a single cysteine residue (129W/152C). In the mutant, the endogenous Trp192 was changed to Phe and the two endogenous Cys81 and Cys98 were mutated to Ser and Ile, respectively. Similar mutations were previously found to have a minimal effect on the functional properties of cTnI.[27] The mutant clone construction, protein expression, purification, and characterization were carried out as in our previous work.[27] The single cysteine residue in the cTnI mutant was labeled with IAEDANS in the presence of 6 M urea,[28] and degree of labeling was found to be >0.97 mol probe/mol of protein. Reconstitution of the cTnI mutant with wild-type cTnC into the binary complex and with the tryptophanless cTnT mutant into the ternary troponin complex was carried out by incubation of the proteins at 4 °C in the presence of 6 M urea at the ratio of [cTnI]:[cTnC] = 1:3 for the binary complex, and [cTnI]:[cTnT]:[cTnC] = 1:1.2:3 for the ternary complex. The incubation mixture also contained 30 mM Mops at pH 7.2, 1 mM DTT, and 50 mM Ca^{2+}. A step-wise exhaustive dialysis was used to remove urea and renature the complexes.[29] The final sample was dialyzed against a working buffer containing 50 mM Mops at pH 7.2, 1 mM DTT, 1 mM EGTA, 5 mM $MgCl_2$, and 0.2 M KCl. Protein concentrations were determined by the Bradford method. A Ca^{2+} titration of the ternary complex formed between a fluorescently labeled cTnC and the mutant cTnI plus wild-type cTnT was carried out as previously described.[29] The titration curve was monophasic with a pCa value of 5.85 as the apparent Ca^{2+} affinity for this complex. The pCa value determined with a ternary complex formed with wild-type cTnI was 5.70 and with a previous cTnI mutant was 5.81. Upon reconstitution into myofibrils, the previous cTnI mutant was found to have a Ca^{2+}-dependent myofibrillar ATPase activity within 2% of the wild-type cTnI.[27] Thus, the mutant cTnI used here was

judged not to be functionally altered in any significantly way.

Fluorescence measurements

Steady-state fluorescence measurements were carried out at 20(±0.1) °C on an ISS PC1 photon-counting spectrofluorometer, using a band pass of 3 nm on both the excitation and emission monochromators. Emission spectra were recorded with the proteins in the working buffer and were corrected for variation of the detector system with wavelength. For each emission spectrum, the background signal was corrected using solutions in which proteins were omitted. Protein concentration was 5 μM for all spectral measurements. When Ca^{2+} was present, the total concentration was 3 mM. The quantum yield of cTnI Trp129 was determined by the comparative method.[30]

Fluorescence intensity decays and anisotropy decays were measured at 20(±0.1) °C in the time domain with either a PRA 3000 single photon-counting lifetime spectrometer equipped with a rhodamine 6G dye laser cavity dumped and synchronously pumped by a mode locked argon ion laser[30] or an IBH 5000 photon-counting lifetime system equipped with a very stable flash lamp operated at 40 kHz in 0.5 atm of hydrogen. For FRET measurements with mutant cTnI, the donor was the Trp129 and the acceptor was the extrinsic fluorophore AEDANS covalently linked to the single Cys152. The excitation wavelength was 295 nm and the emission wavelength was 333 nm for tryptophan, and the corresponding wavelengths for AEDANS were 330 nm and 480 nm, respectively. Fluorescence intensity decays of the donor from the donor-alone and donor-acceptor samples were collected into 1024 channels of a multichannel analyzer (PCA3) under identical experimental condition and used to calculate the distribution of the intersite distances between donor and acceptor as described.[28,31] The decay profiles were corrected for background signals using an identical solution in which the cTnI component was omitted. Anisotropy decays of both donor and acceptor were determined using vertically polarized excitation and measuring the emission polarized in the vertical and horizontal directions. The anisotropy decay data were fitted to a sum of two exponential terms to recover the limiting anisotropies at zero time.[28]

Acknowledgments

We thank Dr Paul R. Rosevear for useful discussions and comments on the preparation of this manuscript. This work was supported by a grant from the US National Institutes of Health (HL52508).

References

1. Satyshur, K. A., Rao, S. T., Pyzalska, D., Drendel, W., Greaser, M. & Sundaralingam, M. (1988). Refined structure of chicken skeletal muscle troponin C in the two-calcium state at 2 Å resolution. *J. Biol. Chem,* **263**, 1628-1647.
2. Herzberg, O. & James, M. N. G. (1988). Refined crystal structure of troponin C from turkey skeletal muscle at 2.0 Å resolution. *J. Mol. Biol.* **203**, 761-779.
3. Houdusse, A., Love, M. L., Dominguez, R., Grabarek, Z. & Cohen, C. (1997). Structures of $4Ca^{2+}$-bound troponin C at 2.0 Å resolution: Further insights into the Ca^{2+}-switch in the calmodulin superfamily. *Structure,* **5**, 1695-1711.
4. Putkey, J. A., Liu, W. & Sweeney, H. L. (1991). Function of the N-terminal calcium-binding sites in cardiac/slow troponin C assessed in fast skeletal muscle fibers. *J. Biol. Chem.* **266**, 14881-14884.
5. Dong, W.-J., Xing, J., Villain, M., Hellinger, M., Robinson, J. M., Chandra, M. *et al*. (1999). Conformation of the regulatory domain of cardiac muscle troponin C in its complex with cardiac troponin I. *J. Biol. Chem.* **274**, 31382-31390.
6. Li, M. X., Spyracopoulos, L. & Sykes, B. D. (1999). Binding of cardiac troponin-$I_{147-163}$ induces a structural opening in human cardiac troponin-C. *Biochemistry,* **38**, 8289-8298.
7. Syska, H., Wilkinson, J. M., Grand, R. J. & Perry, S. V. (1976). The relationship between biological activity and primary structure of troponin I from white skeletal muscle of the rabbit. *Biochem. J.* **153**, 375-387.
8. Talbot, J. A. & Hodges, R. S. (1981). Comparative studies on the inhibitory region of selected species of troponin-I. The use of synthetic peptide analogs to probe structure-function relationships. *J. Biol. Chem.* **256**, 2798-2802.
9. Olah, G. A. & Trewhella, J. (1994). A model structure of the muscle protein complex $4Ca^{2+}$- troponin C/troponin I derived from small-angle scattering data: implications for regulation. *Biochemistry,* **33**, 12800-12806.
10. Stone, D. B., Timmins, P. A., Schneider, D. K., Krylova, I., Ramos, C. H., Reinach, F. C. & Mendelson, R. A. (1998). The effect of regulatory Ca^{2+} on the *in situ* structures of troponin C and troponin I: a neutron scattering study. *J. Mol. Biol.* **281**, 689-704.
11. Luo, Y., Wu, J. L., Li, B., Langsetmo, K., Gergely, J. & Tao, T. (2000). Photocrosslinking of benzophenone-labeled single cysteine troponin I mutants to other thin filament proteins. *J. Mol. Biol.* **296**, 899-910.
12. Tung, C. S., Wall, M. E., Gallagher, S. C. & Trewhella, J. (2000). A model of troponin-I in complex with troponin-C using hybrid experimental data: the inhibitory region is a beta-hairpin. *Protein Sci.* **9**, 1312-1326.
13. Dong, W.-J., Xing, J., Chandra, M., Solaro, R. J. & Cheung, H. C. (2000). Structural mapping of single cysteine mutants of cardiac troponin I. *Proteins: Struct. Funct. Genet.* **41**, 438-447.
14. Straume, M., Fraser-Cadoret, S. G. & Johnson, M. L. (1991). Least-squares analysis of fluorescence data. In *Topics in Fluorescence Spectroscopy* (Lakowicz, J. R., ed.), vol. 2, pp. 177-239, Plenum Press, New York.
15. Cheung, H. C., Wang, C.-K., Gryczynski, I., Wiczk, W., Laczko, G., Johnson, M. L. & Lakowicz, J. R. (1991). Distance distributions and anisotropy decays of troponin C and its complexes with troponin I. *Biochemistry,* **30**, 5238-5247.
16. Dale, R. E., Eisinger, J. & Blumberg, W. E. (1979). The orientational freedom of molecular probes. The orientation factor in intramolecular energy transfer. *Biophys. J.* **26**, 161-193.
17. Howarth, J. W., Krudy, G. A., Lin, X., Putkey, J. A. & Rosevear, P. R. (1995). An NMR and spin label study of the effects of binding calcium and troponin

I inhibitory peptide to cardiac troponin C. *Protein Sci.* **4**, 671-680.
18. Pearlstone, J. R. & Smillie, L. B. (1995). Evidence for 2-site binding of troponin-I inhibitory peptides to the N-domain and C-domain of troponin-C. *Biochemistry,* **34**, 6932-6940.
19. McKay, R. T., Tripet, B. P., Hodges, R. S. & Sykes, B. D. (1997). Interaction of the second binding region of troponin I with the regulatory domain of skeletal muscle troponin C as determined by NMR spectroscopy. *J. Biol. Chem.* **272**, 2894-2850.
20. Tripet, B., Van Eyk, J. E. & Hodges, R. S. (1997). Mapping of a second actin-tropomyosin and a second troponin C binding site within the C terminus of troponin I, and their importance in the Ca^{2+}-dependent regulation of muscle contraction. *J. Mol. Biol.* **271**, 728-750.
21. Campbell, P. A. & Sykes, B. D. (1991). Interaction of troponin I. Use of the two-dimensional nuclear magnetic resonance transferred nuclear Overhauser effect to determine the structure of the inhibitory troponin I peptide when bound to skeletal troponin C. *J. Mol. Biol.* **222**, 405-421.
22. Hernαndez, G., Blumenthal, D. K., Kennedy, M. A., Unkefer, C. J. & Trewhella, J. (1999). Troponin I inhibitory peptide (96-115) has an extended conformation when bound to skeletal muscle troponin C. *Biochemistry,* **38**, 6911-6917.
23. Abbotts, M. B., Dvoretsky, A., Gaponenko, V. & Rosevear, P. R. (2000). Cardiac troponin I inhibitory peptide: location of interaction sites on troponin C. *FEBS Letters,* **409**, 168-172.
24. Abbots, M. B., Dong, W.-J., Dvoretsky, A., DaGue, B., Caprioli, R. M., Cheung, H. C. & Rosevear, P. R. (2001). Modulation of cardiac troponin C-cardiac troponin I regulatory interactions by the amino-terminus of cardiac troponin I. *Biochemistry,* **40**, 5992-6001.
25. Xing, J., Dong, W.-J., Chandra, R., Solaro, R. J., Umeda, P. K. & Cheung, H. C. (1999). Proximity mapping of the cardiac cTnC-cTnI complex. *Biophys. J.* **76**, A279.
26. She, M., Dong, W.-J., Umeda, P. K. & Cheung, H. C. (1998). Tryptophan mutants of troponin C from skeletal muscle. An optical probe of the regulatory domain. *Eur. J. Biochem.* **252**, 600-607.
27. Dong, W.-J., Chandra, M., Xing, J., Solaro, R.-J. & Cheung, H. C. (1997). Conformation of the N-terminal segment of a monocysteine mutant of troponin I from cardiac muscle. *Biochemistry,* **36**, 6745-6753.
28. She, M., Xing, J., Dong, W.-J., Umeda, P. K. & Cheung, H. C. (1998). Calcium binding to the regulatory domain of skeletal muscle troponin C induces a highly constrained open conformation. *J. Mol. Biol.* **281**, 445-452.
29. Dong, W.-J., Wang, C.-K., Gordon, A.-M. & Cheung, H. C. (1997). Disparate fluorescence properties of 2-[4′-(iodoacetamido)anilino]-naphthalene-6-sulfonic acid attached to Cys-84 and Cys-35 of troponin C in cardiac muscle troponin. *Biophys. J.* **72**, 850-857.
30. She, M., Dong, W.-J., Umeda, P. K. & Cheung, H. C. (1997). Time-resolved fluorescence study of the single tryptophans of engineered skeletal muscle troponin C. *Biophys. J.* **73**, 1042-1055.
31. Dong, W-. J., Chandra, M., Xing, J., She, M., Solaro, R. J. & Cheung, H. C. (1997). Phosphorylation-induced distance change in a cardiac muscle troponin I mutant. *Biochemistry,* **36**, 6754-6761.

Edited by M. F. Moody

(Received 7 June 2001; received in revised form 21 September 2001; accepted 21 September 2001)